A solid-phase compatible silane-based cleavable linker enables custom isobaric quantitative chemoproteomics

Nikolas R. Burton[‡†], Daniel A. Polasky[`], Flowreen Shikwana[‡†], Samuel Ofori[†], Tianyang Yan[‡†], Daniel J. Geiszler[^], Felipe da Veiga Leprevost[`], Alexey I. Nesvizhskii[`^], and Keriann M. Backus[‡†§‖⊥#*]

† Department of Biological Chemistry, David Geffen School of Medicine, UCLA, Los Angeles, California 90095, United States

‡ Department of Chemistry and Biochemistry, UCLA, Los Angeles, CA, 90095, United States

§ Molecular Biology Institute, UCLA, Los Angeles, California 90095, United States

‖ DOE Institute for Genomics and Proteomics, UCLA, Los Angeles, California 90095, United States

⊥ Eli and Edythe Broad Center of Regenerative Medicine and Stem Cell Research, UCLA, Los Angeles, California 90095, United States

Jonsson Comprehensive Cancer Center, UCLA, Los Angeles, California 90095, United States

^ Department of Computational Medicine and Bioinformatics, University of Michigan, Ann Arbor, Michigan 48109, United States

`Department of Pathology, University of Michigan, Ann Arbor, Michigan 48109, United States

*Corresponding Author: Keriann M. Backus, Biological Chemistry Department, David Geffen School of Medicine, UCLA, Los Angeles, CA, 90095, USA, E-mail: kbackus@mednet.ucla.edu.

ABSTRACT

The human proteome harbors tens of thousands of ligandable or potentially druggable cysteine residues. Consequently, pinpointing the optimal covalent molecule for each cysteine residue is a key challenge for chemical probe and drug discovery campaigns. While chemoproteomic methods have enabled proteome-wide screens of electrophilic molecules, achieving comprehensive proteome-wide structure activity relationship (SAR) maps requires technical innovation in two key areas: (1) streamlined sample preparation workflows and (2) increased sample throughput via multiplexing. Recent inroads in the latter challenge have been made through the incorporation of isobaric tandem mass tags (TMT) into chemoproteomic workflows; the high cost and late-stage isobaric labeling collectively have, however, limited adoption of such MS2/MS3-based quantitation strategies. Here we report the silane-based Cleavable Linkers for Isotopically-labeled Proteomics (sCLIP) method, which harnesses custom isotopically labeled chemoproteomic capture reagents to simplify sample preparation and achieve low cost 6-plex isobaric multiplexing. The sCLIP method is enabled by a high yielding and scalable route to dialkoxydiphenylsilane fluorenylmethyloxycarbonyl (DADPS-Fmoc) protected amino acid building blocks, which enable facile synthesis of customizable, isotopically labeled, and chemically cleavable biotin capture reagents. Benchmarking of a panel of fully functionalized sCLIP capture reagents revealed performance comparable to established platforms. Using the diagnostic ion mining of the FragPipe computational pipeline, we identified a characteristic fragment ion with suitable intensity and specificity for tandem mass spectrometry (MS2)-based quantification. By harnessing this unprecedented gas phase chemistry, we established a cost-effective high performance 6-plex isobaric reagent set in which the mass balancer and reporter are encoded in the cysteine-capping and biotin capture reagents, respectively. Application of the sCLIP reagents to chemoproteomic analysis of electrophilic molecules uncovered 4805 total ligandable cysteines, including established and unprecedented cysteine-ligand pairs.

INTRODUCTION

Mass spectrometry-based chemoproteomics has emerged as enabling technology for functional biology and drug discovery. Showcasing this widespread utility, recent chemoproteomic studies have uncovered covalent degraders[1–6], protein-protein interaction (PPI) modulators[7–9], novel targets with anti-bacterial activity[10–13], pinpointed redox sensitive cysteines[14–17], and have shed light on the mode of action and off-targets of existing drugs and clinical candidates[18–21]. Chemoproteomics has proven useful for identifying both reversible and irreversible protein modulators, including those identified through screens of cysteine-reactive electrophilic fragments[22–25], fully functionalized fragments[26–29], and latent electrophiles[30–32]. Chemical probes compatible with chemoproteomics have been developed that target nearly all nucleophilic amino acid side chains, including serine[33–35], lysine[8], tyrosine[30,36], methionine[37], glutamate and aspartate[38–40], Arginine[41], and cysteine[23,42]. Enabled by this plethora of useful chemistries, an ongoing challenge for the field of chemoproteomics is to fully establish the scope of residues and proteins that can be targeted by chemical probes.

Achieving this ambitious goal, which aligns with the Target2035 objectives[43,44], requires the establishment of robust, streamlined, cost-effective, high throughput, and high coverage chemoproteomic platforms capable of comprehensively surveying the targetable proteome. Significant inroads have already been made into realizing this vision. Recent work, including our own, has demonstrated that by using new ultra-fast mass spectrometers, on-line and off-line fractionation[22,45,46], and improved sample preparation and bioinformatics workflows[47], enhanced coverage of the cysteinome can be achieved. In fact, >25% of all cysteines in the human proteome have now been assayed by chemoproteomics[48].While these technical advances will almost undoubtedly extend to other chemoproteomic modalities, cysteine-centric studies remain a mainstay of chemoproteomics due both the important functional roles cysteines play in proteins

and the proven utility of cysteine-reactive molecules as clinical candidates and even FDA-approved drugs.

Established cysteine chemoproteomic platforms nearly all rely on the same general workflow that includes: (1) cysteine biotinylation (2) isotopic labeling, (3) enrichment and subsequent release of biotinylated peptides from avidin resin, and (4) liquid chromatography–tandem mass spectrometry (LC-MS/MS) analysis. Despite these shared features, established platforms vary in the choice of enrichment handle, for example either iodoacetamide alkyne (IAA), iodoacetamide desthiobiotin (IA-DTB)[22,25], or more tailored labeling reagents, such as hypervalent iodine probes[49–51] and heteroaromatic azoline thioethers (HATs)[52]. Isotopic labeling strategies have emerged as another area of considerable innovation for cysteine chemoproteomics. Gold-standard methods, such as the isotopic tandem orthogonal proteolysis activity-based protein profiling (isoTOP-ABPP) workflow[42] (**Figure 1A**) and the more recent related methods isotopically labeled desthiobiotin azide (isoDTB)[10] have relied heavily on the incorporation of isotopic labels into chemoproteomic enrichment handles.

Given the high cost of isotopically labeled building blocks, isotopically labeled chemoproteomic capture reagents are frequently synthesized via solid phase routes, which benefit from the near quantitative yields and ease of purification and isotope incorporation. Exemplifying these reagents, isoTOP-ABPP utilizes isotopically differentiated tobacco etch virus (TEV)-cleavable azidobiotin peptide capture reagents synthesized through solid-phase peptide synthesis (SPPS). A +6 Da mass difference between "heavy" and "light" reagents, achieved via $^{13}C_5,^{15}N$-Valine incorporation, allows for precursor-based (MS1) quantification of treatment-induced changes to heavy- versus light-labeled peptide abundance.

Chemoproteomic studies, including our own[15,17,47,48,53–55], continue to rely on stable isotope incorporation, either through metabolic labeling or the aforementioned custom isotopically labeled capture reagents, and MS1 based quantification[10,42,56–58]. These methods are widely adopted in large part due to their relatively reasonable cost, the compatibility of the resulting datasets with

freely available software packages for analysis[59–61], and increased data reproducibility afforded by the ability to combine 'treated' and 'control' samples early in the sample preparation workflow. More recent work has demonstrated that quantification of cysteine chemoproteomic datasets can also be achieved using label free quantification (LFQ), including data dependent studies (DDA) that utilize FragPipe computational platform with MSFragger and IonQuant[15,62]and data independent analysis (DIA) that uses Spectronaut[63].

Due to the limits of multiplexing with MS1-based quantification, the sample throughput of the aforementioned methods remains comparably modest. Isobaric labeling using tandem mass tag (TMT) reagents has emerged as an attractive alternative to MS1-based quantification methods, which enables high coverage sample multiplexing[64,65]. Applications of TMT to cysteine chemoproteomics has enabled the proteome-wide identification of ligandable and reactive cysteines in immune cells and the high throughput screening of comparatively large compound libraries[22,25,26,66].

Despite these considerable advances, there remain several unmet needs for multiplexed chemoproteomics. First, the development of lower cost isobaric reagents would increase community-wide adoption of multiplexing workflows. Second, while the use of isobaric reagents substantially decreases acquisition time, such labeling strategies do not afford a similar decrease in sample preparation time—isobaric labeling is performed after sequence specific proteolysis, comparatively late in sample preparation workflows. Consequently, there is an unmet need for development of isobaric capture reagents, which allow for earlier sample combination and consequently more streamlined sample preparation. Such reagents, in many ways analogous to iodo-TMT-based platforms that harness an anti-TMT antibody to capture cysteine peptides[67,68], would offer the added advantage of universal compatibility with alkyne-based probes and thus ready compatibility beyond cysteine chemoproteomics.

Here, we achieve both reduced isobaric reagent cost and streamlined sample preparation workflows by developing the silane-based Cleavable Linkers for Isotopically-labeled Proteomics

(sCLIP) method. To establish sCLIP, we first developed a robust and high yielding synthetic route to obtain two versatile dialkoxydiphenylsilane (DADPS) and fluorenylmethyl carbamate (Fmoc) functionalized building blocks (DADPS-Fmoc reagents), which function analogously to Fmoc-protected amino acids commonly utilized in SPPS. We chose to focus on the DADPS group, due to the mild MS-compatible cleavage conditions (2% formic acid), compatibility with all sequence specific proteases, and previously reported superior proteomic performance when compared with other commonly employed cleavable linkers[69–71]. Highlighting the synthetic and chemoproteomic utility of the innovative DADPS-Fmoc reagents, a panel of chemically cleavable chemoproteomics capture reagents was obtained in high yield and purity via SPPS, including isotopically differentiated (light and heavy) reagents obtained with low-cost building blocks (**Figure 1B**). FragPipe with MSFragger labile search[72] and PTM-Shepherd diagnostic feature detection[73] revealed a high intensity and highly specific dihydrooxazolium ion unique to a subset of sCLIP reagents. By harnessing this dihydrooxazolium ion, we developed the sCLIP isobaric platform, which is a low cost six-plex isobaric labeling strategy in which the mass balancer and reporter are incorporated into cysteine-reactive iodoacetamide alkyne probe and sCLIP capture reagent, respectively (**Figure 1C**). Application of sCLIP to cysteine chemoproteomics revealed comparable performance to TMT and compatibility with screening known and novel cysteine reactive electrophiles, including the discovery that the mitochondrial uncoupling agent Carbonyl cyanide-p-trifluoromethoxyphenylhydrazone (FCCP)[74] functions as a heretofore unreported covalent-reversible cysteine-reactive electrophile.

Figure 1. Solid phase peptide synthesis (SPPS) enables the synthesis of (A) previously synthesized isotopic Tandem Orthogonal Proteolysis–Activity-Based Protein Profiling (isoTOP-ABPP)[42] and (B) our silane-based Cleavable Linker for Isotopically-labeled Proteomics (sCLIP) capture reagents. (C) sCLIP chemoproteomic platform for profiling ligandable cysteines. Cysteines are capped with isotopically labeled iodoacetamide alkyne (IAA) pan-cysteine

alkylation reagents to act as a balancer for MS2 quantification. Labeled cysteines are then click-conjugated to isotopically labeled sCLIP capture reagents. Either MS1 or MS2 level quantification (reagent choice dependent) are achieved after sample pooling and single-pot, solid-phase enhanced sample preparation coupled with high field asymmetric waveform ion mobility spectrometry (SP3-FAIMS)[47,54] and analysis. MS2-level quantification is enabled by gas-phase reagent fragmentation of the triazole moiety releasing a dihydrooxazolium reporter ion, which is balanced by isotopically labeled balancer derived from the iodoacetamide alkyne reagents. Red asterisks indicate sites amenable to heavy isotope incorporation.

RESULTS

Establishing a route to a prototype DADPS-Fmoc building block

Despite their favorable properties for chemoproteomics, synthetic strategies for incorporating dialkoxydiphenylsilane (DADPS) moieties into enrichment reagents remain limited, with previously reported reagents requiring multi-step routes that are hindered by the often challenging and inefficient reactions required to form the DADPS linkage[19,75,76]. To address these limitations, we envisioned building DADPS-containing chemoproteomic capture reagents via SPPS, starting from a DADPS-Fmoc solid-phase compatible building block. However, to our knowledge, DADPS incorporation into polypeptides obtained through SPPS remains largely unexplored, although prior implementation of silyl moieties for capture and release of cargo supported feasibility[77,78].

Therefore, our first step was to develop a high yielding and robust synthetic route to access a DADPS-Fmoc reagent that could function analogously to a protected amino acid, with the twin goals of testing SPPS compatibility and streamlining chemoproteomic capture reagent synthesis. With the goal of minimal protecting group manipulation, we first tested DADPS formation between unprotected β-hydroxyisovaleric acid **S1** with a protected amino alcohol **S2**. Under all reaction conditions tested, we observed none of the desired product and instead observed homo coupling

of the primary alcohol (**Scheme S1**). By comparison, DADPS formation proceeded efficiently for the model reaction between alcohol **S2** and α,α-dimethylphenethanol, which lacks a free acid. This model reaction also revealed that increased yields could be achieved with addition of 4-dimethylaminopyridine (DMAP), which made the synthetic route incompatible with direct use of Fmoc-protected amines (**Scheme S2**)[79,80].

We next opted to generate ester protected substrates to more fully probe whether DADPS reagents could be obtained for substrates lacking the free acid. DADPS formation proceeded smoothly for a panel of protected β-hydroxyisovalerate analogues **S6-S10**, affording the desired products **S12-S17** in moderate to high yields (**Scheme S3**). However, subsequent ester deprotection under all conditions evaluated failed to afford the desired acid product **S29** (**Table S1**). We therefore next investigated whether DADPS reagents featuring activated acyl moieties could be synthesized, as such substrates would obviate the need for subsequent ester deprotection. Following established conditions, we obtained a panel of five β-hydroxyisovaleric acid analogues **S18-S22** (**Scheme S4**) in near quantitative yields (78-99%). Unfortunately, subsequent DADPS formation afforded none of the desired products, likely due to immediate attack of the activated acyl group by the primary alcohol (**Scheme S5**). Further attempts to perform this reaction with weaker bases resulted in trace product **S23** (**Scheme S6**).

Synthesis and validation of solid phase compatibility of the DADPS-Fmoc reagents 8 and 9.

Given the generally mild and orthogonal conditions required for thiol-ene chemistry and the availability of our allyl ester model substrate **S7**, we tested whether **S7** could be coupled to 3-mercaptopropionic acid (MPA) under photoinitiated reaction conditions. Gratifyingly, we obtained the desired thioether in 61% yield (**Scheme S7A**). However, all efforts towards selective deprotection of the Cbz group in the presence of the allyl ester were unproductive (**Scheme S7B**). We therefore replaced the Cbz with phthalimide protected amine **3**, which afforded allyl ester

DADPS reagent **S26** in 92% yield. Subsequent protecting group manipulation afforded Fmoc protected DADPS reagent, **S27**, in 70% yield over two steps (**Scheme S8**).

We next subjected **S27** to a photoinitiated thiol-ene reaction with MPA to form a thioether linkage and free carboxylic acid on the reagent, obtaining our first solid phase compatible DADPS reagent **S28** in 59% yield (**Scheme S8**). While the high yield formation of this model substrate was encouraging, we opted to modify our strategy slightly to eliminate the ester moiety, due to its potential hydrolytic instability in esterase containing cell lysates. Additionally, we were concerned about the aqueous buffer solubility of our reagent bearing the long hexyl chain. This led us to repeat the sequence of DADPS formation with an allyl ether and making two reagents **8** and **9**, which differed by alkyl chain length. Notably, the thiol-ene was performed neat as previously reported[81], providing the final solid-phase compatible reagent in 39% yield for the reagent bearing an ethyl chain **8** and 31% yield for the hexyl chain **9** over 4 steps. Further reference to DADPS reagents refers to solid-phase compatible building blocks **8** and **9** (**Scheme 1**).
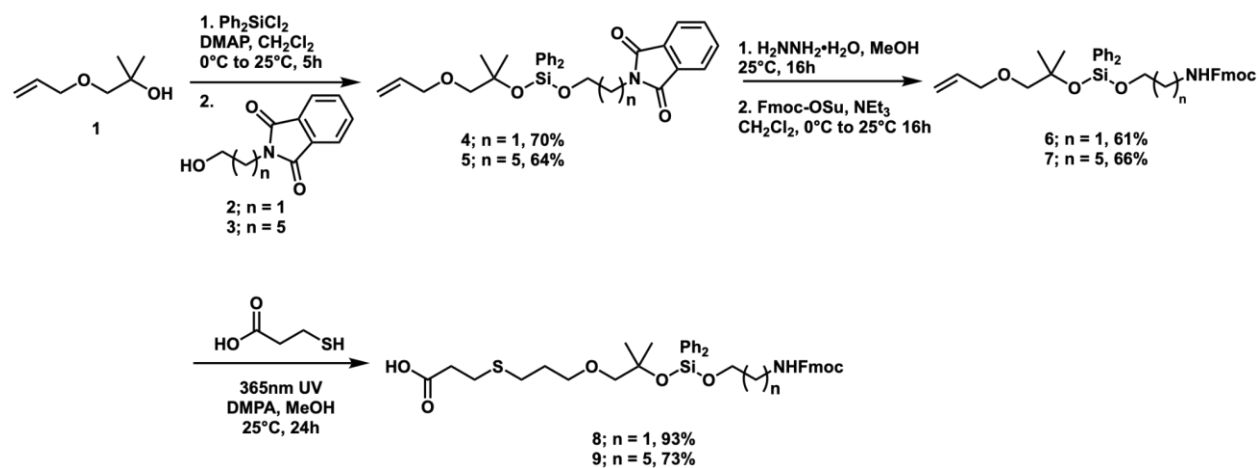
Scheme 1. Synthesis of solid-phase compatible DADPS-Fmoc reagents **8** and **9,** which were obtained in 39% and 31% overall yields, respectively
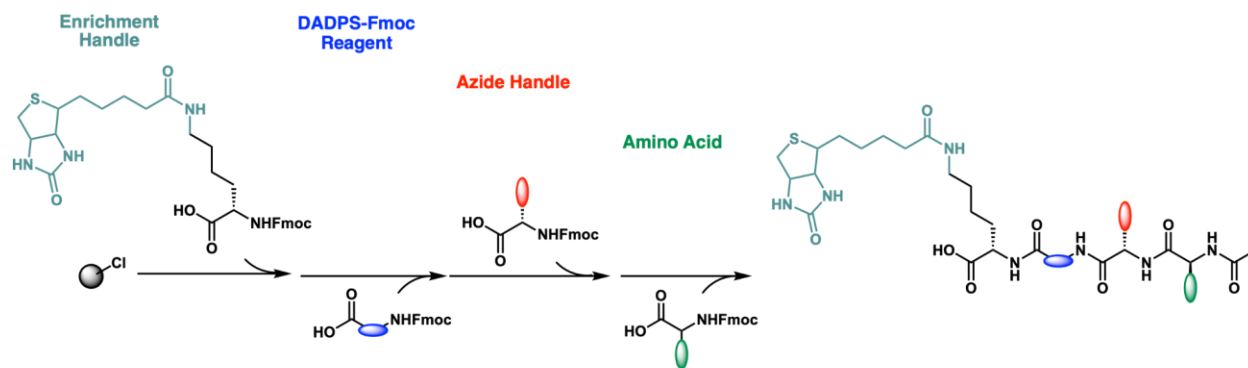
sCLIP Tag	DADPS Reagent	Azide Handle	Amino Acid	Yield
10	8	Lys-N$_3$	L-Valine	43%
11	8	Lys-N$_3$	L-Alanine	59%
12	9	Lys-N$_3$	L-Valine	46%
13	8	ß-N$_3$-Ala	L-Valine	61%
14	8	Lys-N$_3$	L-Valine ($^{13}C_5$, ^{15}N)	58%
15	9	ß-N$_3$-Ala	L-Valine	40%
16	9	ß-N$_3$-Ala	L-Alanine	50%

Figure 2. Our approach utilizes a solid-phase compatible DADPS-fmoc reagent for high yielding synthesis of our silane Cleavable Linkers for Isotopic Proteomics (sCLIP) chemoproteomic capture reagents. Yields for the preparation of prototype DADPS-containing capture reagents with different i) SPPS-compatible DADPS reagent (blue); ii) Azide Handle (red); and iii) Amino Acid (green) on the N-terminus.

Solid phase synthesis (SPS) and proteomic benchmarking of a panel of DADPS functionalized chemoproteomics capture reagents 10, 11, 12, and 13.

With a working route for DADPS reagent synthesis in hand, our next step was to synthesize a panel of chemoproteomic capture reagents which we will refer to as silane Cleavable Linkers for Isotopic Proteomics (sCLIP) chemoproteomic capture reagents (**Figure 2** and **Figure S1**). We

opted to focus on exploring three variables: the linker length, the source of azide, and nature of the amino acid used for isotopically labeled reagent synthesis. We prioritized linker length as we wanted to assess how changes to the reagent size would impact proteomic coverage. For azide source, we chose to compare ß-azidoalanine with azidolysine with the goals of determining how reducing the reagent size would impact proteomic coverage and click efficiency, together with assessing how triazole fragmentation would be impacted by choice of azide. Our prior study[55] had revealed that the gas phase fragmentation of triazole modified peptides produced signature fragment ions, with the identity, intensity, and specificity of the produced ions varying depending on the nature of the azide. Therefore, we speculated that we might observe differences in the fragmentation pattern of azidohomoalanine and azidolysine based reagents, which could be harnessed for the production of a novel isobaric labeling strategy. Lastly, given the ready availability of various isotopically labeled amino acids, most notably valine and alanine, we wanted to assess whether incorporation of isotopically labeled amino acids into our reagents would enable MS1 or MS2-based quantification and whether amino acid selection would impact reagent performance.

With these objectives in mind, we synthesized a panel of four test reagents (**Figure 2** and **Figure S1**; **10, 11, 12,** and **13**), which were obtained in high yield and purity, with the goal of systematically comparing each of the aforementioned variables. Using HEK293T cell lysates, we established a prototype sCLIP workflow to enrich labeled peptides. For sCLIP capture, we identified cysteine-containing peptides, using a modified version of our single-pot, solid-phase, enhanced sample-preparation (SP3) workflow[47] for analysis of the cysteinome (**Figure 3A**). First cysteines were capped with the highly reactive cysteine alkylating reagent iodoacetamide alkyne (**Figure S1;** IAA). The alkyne-labeled lysates were then subjected to click conditions with each of our sCLIP capture reagents followed by SP3 sample cleanup, tryptic digest, capture of labeled peptides with streptavidin resin, and release of labeled peptides under mild acidic conditions. LC-MS/MS analysis revealed similar performance for all reagents, as indicated by the comparable

numbers of peptide spectral matches (PSMs), peptides, and protein identifications across the panel, with modestly increased coverage observed for reagent **13** (**Figure 3B**). Performance was also comparable to samples prepared using biotin-azide capture and our previously reported workflow (**Figure S2**). We observe comparable performance for the alanine and valine reagents **10** and **11**, indicating that proteomic analysis should proceed smoothly using reagents incorporating either heavy valine or heavy alanine building blocks. High click reaction efficiency was observed across the reagent panel, indicating that the greater steric hindrance of the ß-azidoalanine reagents did not decrease performance as a factor leading to differences in coverage (**Figure 3C**). All reagents also afforded similar coverage to that obtained for samples prepared in parallel using our established biotin-azide capture method (**Figure S4**). Furthermore, across all four reagents we identified 14,456 total cysteines with 10,685 being identified with at least two of the reagents (**Figure 3D**). Of these 14,456 cysteines we compared them to our recently reported cysteine database (CysDB[48]) and found that 803 had not been previously identified (**Figure 3E**).
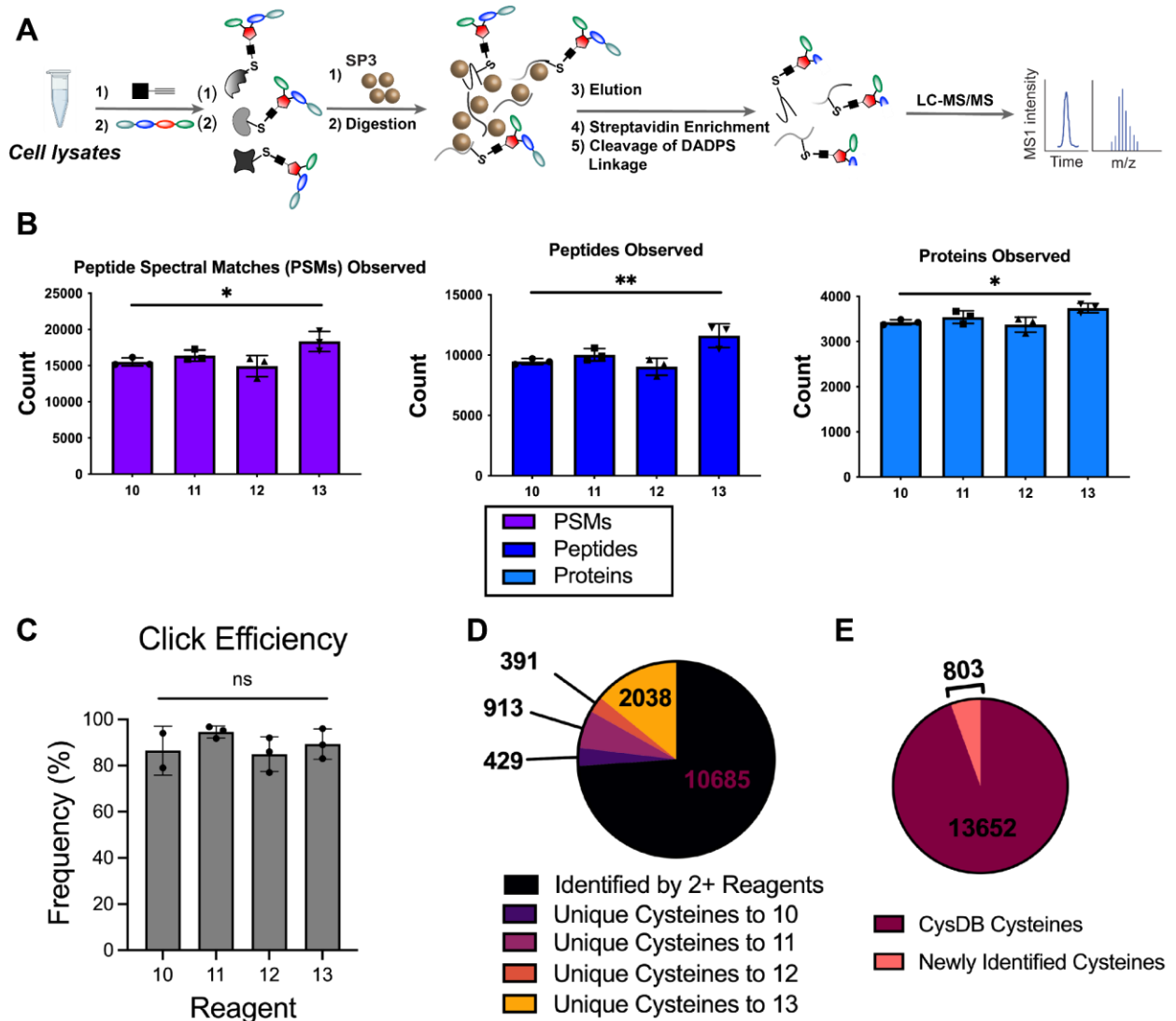
Figure 3. Comparison of sCLIP capture reagents bearing different linkers, azide handles, and N-terminal amino acids. (A) Cysteine profiling workflow with sCLIP reagents. (1) Proteins are first capped with iodoacetamide alkyne (IAA), a pan-reactive cysteine probe. (2) Labeled proteins are then clicked to an sCLIP reagent. Following SP3 sample cleanup, digestion, and streptavidin enrichment, peptides are cleaved off of resin at the DADPS moiety and analyzed by LC-MS/MS analysis. (B) PSMs, unique peptides, and proteins identified by samples prepared using IAA and DADPS azide capture reagents **10, 11**, **12**, and **13**. (C) Click efficiency was calculated through analysis of pre-enriched tryptic digests, as the percentage of IAA modified PSMs detected with click conjugation modifications. Statistical significance was calculated with a

one-way ANOVA test, *p < 0.05, **p < 0.01, ***p < 0.001, and NS p > 0.05. (D) Comparison of cysteines identified across the panel of four sCLIP capture reagents. (E) Comparison of all cysteines liganded using reagents **10**-**13** to previously liganded cysteines in the human proteome as identified by CysDB[48]. All MS data can be found in **Table S3**.

FragPipe-enabled PTM-Shepherd diagnostic feature detection of signature fragment ions produced from sCLIP labeled peptides that are compatible with MS2 quantification.

Motivated by our recent use of diagnostic feature detection[73] to identify characteristic fragment ions derived from biotin-modified precursor ions[55], we next subjected our sCLIP datasets to diagnostic feature extraction using FragPipe with MSFragger and PTM-Shepherd (**Figure 4A**). Our objective was to determine whether the sCLIP modified peptides would afford characteristic fragment ions with suitable intensity and specificity to function as diagnostic ions, which would lay the foundation for establishing a customized isobaric platform. For these analyses we added samples prepared using two additional sCLIP reagents to our panel (**Figure 2** and **Figure S1**; **15**, and **16**). Diagnostic feature searches identified a substantial number of characteristic fragment ions (~29-40/reagent) **(Table S4)**. Prioritizing those ions that exhibited both high intensity and frequent detection, we predicted the likely fragmentation pathways for six reagents, **10**, **11**, **12**, **13**, **15**, and **16**, which were selected to test how three parameters: (1) ethyl vs hexylalcohol substituents (**10** vs **12**, and **13** vs **15**, respectively), (2) azidolysine vs ß-azidoalanine enrichment handles (**10-12 vs 13, 15,** and **16** respectively), and (3) alanine versus valine candidate isotopic labeling sites (**10** vs **11** and **15** vs **16**, respectively) would impact the frequency and abundance of detected fragment ions (**Figure 4B, Table S2, Figure S3**).

Using the identified ions, we next re-searched our datasets using MSFragger labile ion search[55,72,82] to pinpoint ions that exhibited both high intensity and high (near 100%) frequency of detection in modified peptide spectra, while simultaneously having low background identification

in unmodified peptide spectra. Exemplifying this process, for **M1** precursors modified with reagent **12** (**Figure 4B**), we identified a characteristic ion with *m/z* 510.3762, which we ascribed to formation of the **F1** ammonium ion through N26-C27 amide bond cleavage. For the remaining five sCLIP reagent precursor ions **M2, M3, M4, M5,** and **M6**, we observed *m/z* values that matched comparable ammonium ions (**F1**, **F5**, **F9**, as shown in **Figure 4B** for hexyl reagents and **F12**, **F17**, and **F21** as shown in **Figure S3** for ethyl reagents). We then compared the frequency of detection and relative intensity of the ammonium ions for MS/MS spectra generated from modified vs unmodified precursor ions (**Figure 4C** and **Figure S4** for hexyl vs ethyl reagents, respectively). Notably, due to the high click efficiency (**Figure 3C**) and streptavidin enrichment step (**Figure 3A**) >80% of all peptides in the samples are sCLIP modified (**Figure S5**); the small fraction of unmodified precursor ions stem from non-specific binding to the streptavidin resin. The frequency of detection of the ammonium species for modified spectra was observed to be generally high (>70%), particularly for the azido-lysine modified precursors **M1**, **M2**, **M4** and **M5**. However, low relative intensity <5% indicated unsuitability for subsequent isobaric reagent development (**Figure 4C** and **Figure S4**). We additionally further validated the presence and intensity of identified ions through manual inspection of individual MS/MS spectra using an integrated proteomics data viewer in FragPipe (FragPipe-PDV[83]) (**Figure 4D**, **Figure S6**, and **Figure S7**).

Extension of these analyses to subsequent ions revealed favorable properties for ions with m/z values corresponding to dihydrooxazolium ions **F6**, **F10,** and **F22,** formed from ß-azidoalanine modified precursors **M2, M3,** and **M6.** These ions are expected to form after C-N bond cleavage of the triazole followed by cyclization with the proximal carbonyl oxygen, analogous to the formation of our previously reported oxonium-biotin characteristic ion[55]. However, unlike the oxonium-biotin fragmentation, which showed both high intensity and low specificity for precursor modification state, for these ions, we observed high precursor ion specificity, as indicated by the high relative median ion intensity (>55%) for modified spectra compared to low intensity (<20%) for unmodified spectra for **F6**, **F10,** and **F22**. Addition of a field

asymmetric ion mobility (+FAIMS) device further improved this specificity, as observed in both the frequency and intensity analysis (**Figure 4C**).

For azidolysine modified precursors **M1, M4,** and **M5,** analogous oxonium species **F2**, **F13,** and **F18** were also detected, albeit with very reduced median ion intensity (<15%), ascribable to disfavorable formation of an eight-membered ring. For both the azidolysine ß-azidoalanine modified precursors **M2, M3, and M6**, we also observed formation of fragment ions with m/z values corresponding to peptide bond cleavage, triazole fragmentation, and cyclization, to afford aziridinium (**F4** and **F8**) and piperidinium (**F15**) species. Formation of **F8** was observed to be sensitive to proximal amino acids, highly disfavored for valine-containing reagents in comparison to alanine-containing reagents. Ions with m/z values matching deacetylation products (**F3**, **F7**, **F11**, **F14**, **F19**, and **F21**) were also observed for all reagents (**Figure 4B**, **Figure 4C**, **Figure S3**, and **Figure S4**). Both sets of ions were observed at lower median intensity when compared with the dihydrooxazolium ions.

Collectively, across all ions analyzed, the **F6** and **F10** dihydrooxazolium ions were distinguished by the combination of near 100% frequency of detection, high intensity and specificity for modified precursors, which was further improved through FAIMS data acquisition. While both the short **13** and long **15** linker reagents produced the dihydrooxazolium ions, we observed modest improvement in the signal to noise ratio for the hexyl reagent **15**, as assayed by fragment ion intensity in modified vs unmodified spectra, of the corresponding ion using the longer linker reagent (**Figure 4C** and **Figure S4**). Only subtle, albeit significant, differences in **F10** ion intensity were observed with stratification based on peptide length or peptide charge (**Figure 4E**), supporting the generalizability of this fragmentation.
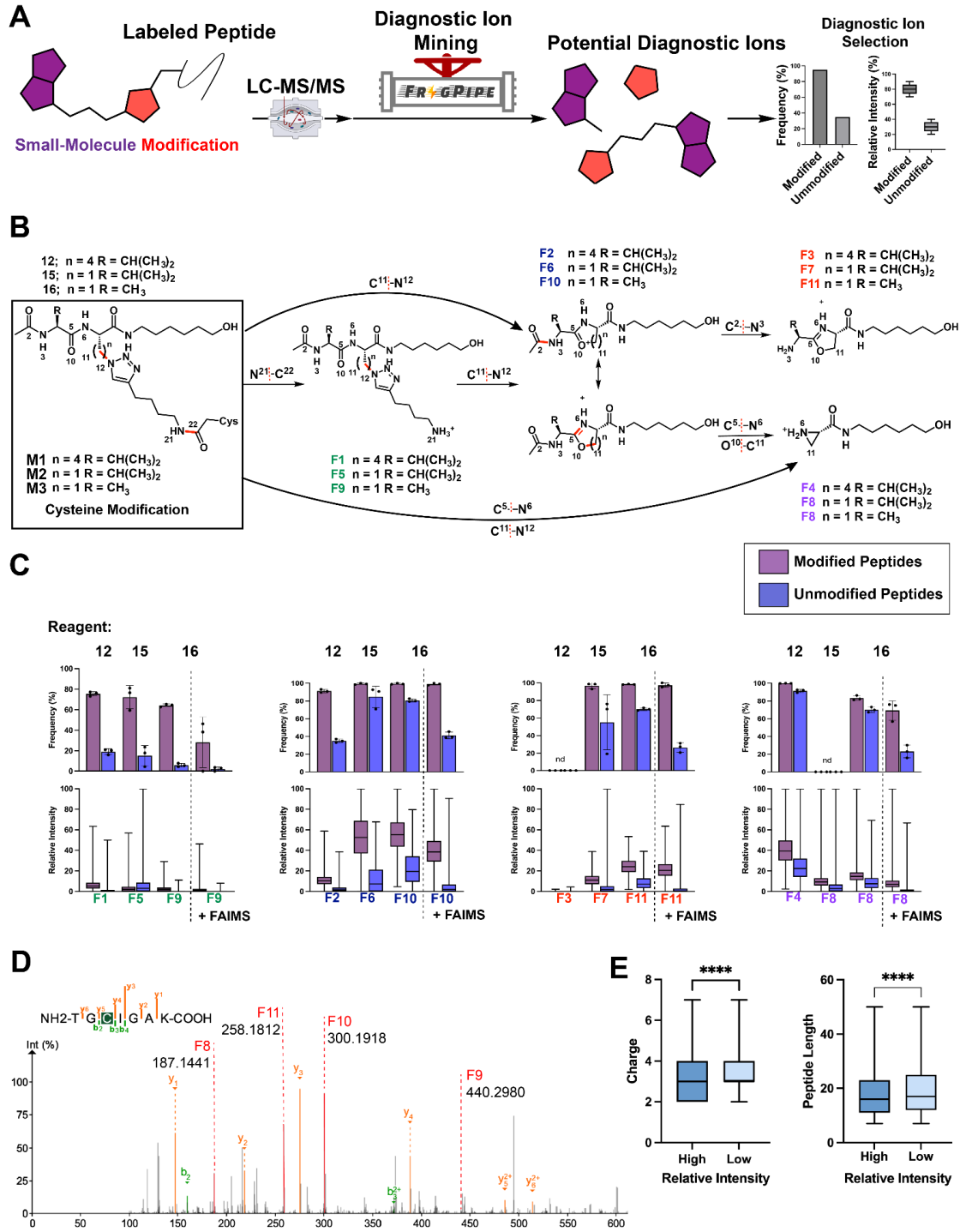
Figure 4. **Diagnostic feature detection identifies a dihydrooxazolium ion as a suitable diagnostic ion for MS² quantitation.** (A) Modified peptides were analyzed using LC-MS/MS and

raw files were analyzed using FragPipe's diagnostic ion mining feature[73]. (B) Predicted fragmentation pattern generated from m/z values identified for diagnostic features identified for peptides modified with sCLIP reagents **12**, **15**, and **16**. (C) Frequency analysis for each fragment ion is shown on the top. Relative intensity I for each fragment ion is shown on the bottom. (D) MS2 spectrum viewed using FragPipe-proteomics data viewer (FragPipe-PDV) for a peptide modified with **16** showing four distinct fragment ions. (E) Peptide charge and length analysis for peptides modified with **16** that produce the **F10** fragment ion. High and low intensity are distinguished as being above or below 50% relative intensity respectively. Statistical significance was calculated with a two-tailed student's t-test, $*p < 0.05$, $**p < 0.01$, $***p < 0.001$, and NS $p > 0.05$. All MS data can be found in **Table S4**.

6-plex isobaric labeling enabled by sCLIP.

Given the ready availability of isotopically differentiated iodoacetamide alkyne reagents, including benzyl-[84] and isopropyl-[17] based reagents, we envisioned the production of a novel isobaric labeling strategy enabled by combining stable isotope labeled iodoacetamide alkyne balancers with sCLIP-generated dihydrooxazolium reporter ions. As a first step to test the feasibility of such a strategy, we subjected sCLIP samples prepared using either benzyl iodoacetamide alkyne (BIAA) or isopropyl iodoacetamide alkyne (IPIAA) for the cysteine capping step, following the workflow shown in **Figure 3A**. Characteristic spectral feature analysis again revealed a substantial number of ions with m/z values matching the predicted fragmentation patterns shown in (**Figures S8-S11).** Both IPIAA and BIAA also did afford fragment ions with m/z values matching oxonium species (**F6, F13, and F18**), albeit with modestly reduced intensities when compared with those generated by IAA. While the azidolysine reagents, when paired with BIAA and IPIAA, did afford an increased intensity for ions with m/z values matching ammonium species, particularly when using the azidolysine sCLIP reagent **11** for sample preparation (**F26, F27, F28, F29, and**

F30), these ions were deemed unsuitable for isobaric reagent development, due to their increased mass and lack of convenient options for obtaining >4-plex multiplexing.

Guided by our extensive fragment ion analysis, we next chose to synthesize a six-plex isobaric reagent set comprised of three custom isotopically differentiated iodoacetamide alkyne balancers (**Figure 5A**, **Figure S12** and **Figure S13**), which would be paired with six isotopically labeled sCLIP reagents, which encode the dihydrooxazolium reporter ions. We opted to use combinations of three heavy isotopes, ^{13}C, ^{18}O, and ^{15}N to generate our six-plex panel of isotopologues (**Figure 5B**), following established precedent for these heavy isotopes being compatible with isobaric labeling strategies[85,86]. IAA isotopologues **23** and **24** were obtained via the respective heavy iodoacetic acid (**Figure S12A**). Following our established solid phase route, sCLIP reagents **16-21** were obtained in high yield and purity (**Figure S12B**). Combination of these IAA and sCLIP reagents yielded a 6-plex set of isobaric reagents (**Figure S12** and **Figure S13**). Additionally, we opted to combine our light sCLIP reagent **16**, with light IAA **22,** to generate an sCLIP zero reagent set for method optimization.

Using the sCLIP zero reagent set to prepare cysteine chemoproteomic samples (following the workflow shown in **Figure 3A**), we next performed a collision energy (CE) ramping experiment. 30% MS^2 higher energy C trap dissociation (HCD) intensity afforded maximum reporter ion intensity with comparable peptide coverage to 25% HCD intensity (**Figure 5C a**nd **Figure 5D**). Given that production of an isobaric label via click chemistry has only limited precedent[87], we next sought to evaluate whether our 6-plex set could generate fragment ions that faithfully report relative precursor ion abundance. To enable quantification of dihydrooxazolium reporter ion intensity, we generated a modified version of Philosopher[88], which added these ions into a custom FragPipe TMT workflow.

We next evaluated whether samples labeled by each of our click-generated isobaric sCLIP reagent pairs (e.g. IAA + sCLIP) would perform comparably for MS2-based quantification, as reported by our custom FragPipe generated reporter ion intensities. We labeled cell lysates in

parallel with each of three isotopically differentiated IAAs followed by click conjugation to equimolar concentration of the complementary sCLIP tag. Analysis of samples combined at a 1:1:1:1:1:1 stoichiometry revealed a median ratio of reporter ion intensity for all reagent pairs centered around one (**Figure 5E**). Ion coalescence was observed at lower resolving powers (RP) for the 302O and 302C channels (**Figure S14**), which we ascribed to their comparatively small 2.5 mDa difference in mass. Because of this small mass difference, analysis of our 6-plex set required an RP of 240K (at m/z 200). This increased resolution and concomitant longer scan time afforded a significant decrease in peptide coverage (**Figure S15**). Consequently, with the goal of maximizing coverage with analysis at 60K RP, we opted to omit the 302O channel from our subsequent analyses. To validate our system's ability to identify peptides at different abundances, we repeated the aforementioned experiment with our 5-plex system, mixing each channel in a 1:4:10:4:1 ratio (**Figure 5F**) and gratifyingly observed median reporter ion ratios closely matching expected intensities corresponding to the channel concentration.
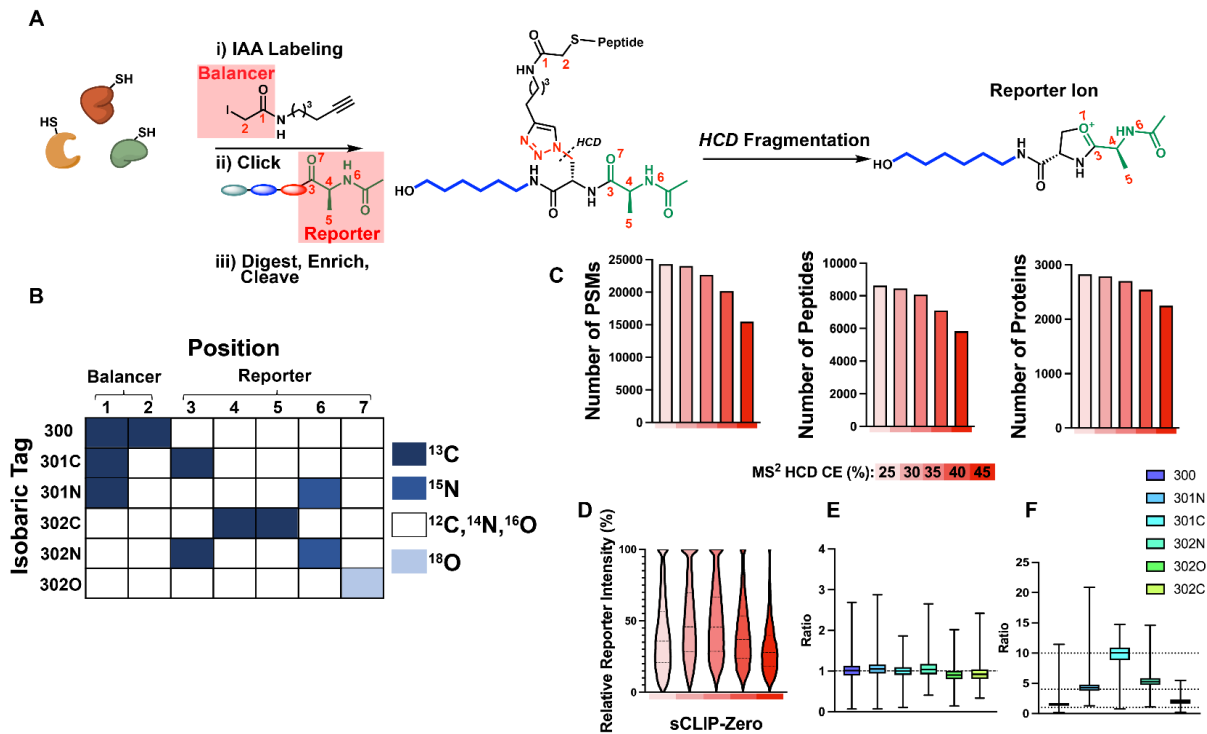
Figure 5. Dihydrooxazolium reporter ion is amenable to MS^2 quantitation. (A) Workflow showing where the balancer section (IAA) and the reporter section (sCLIP) of our isobaric system originate from in a cysteine profiling workflow generating a novel oxazolium reporter ion. (B) Distribution of heavy isotopes for a 6-plex set of isobaric tags. (C) Analysis of PSM, peptide, and protein coverage and (D) fragment Ion intensity for the sCLIP-Zero reagent at varying collision energies. (E) Ratios for each sCLIP channel from samples prepared by mixing all channels of our 6-plex reagent set 1:1 and (F) our 5-plex reagent set in a 1:4:10:4:1 (300:301N:301C:302N:302C) ratio. Box plots display minimum, first quartile (Q1), median, third quartile (Q3), and maximum values of the sample. All MS data can be found in **Table S5**.

Benchmarking sCLIP against TMT

Given the ready availability of widely adopted isobaric reagents, including 6-plex, 10-plex and 16-plex TMT/TMTpro alongside ITRAQ[64,65,89], we next opted to benchmark the sCLIP system against

established reagents. Choosing the widely used 10-plex TMT reagents for comparison, we decide to compare the two workflows for relative ratio compression, coefficient of variance, cost, and coverage. For benchmarking, we opted to prepare two sets of samples in parallel, using isotopically differentiated light and heavy proteomes, generated through Stable Isotopic Labeling by Amino Acids in Cell Culture (SILAC)[56]. Light SILAC lysates were labeled with a 1:10 ratio of the respective isobaric tag reagents (sCLIP/TMT) 301C/128N and 300/127, respectively. In parallel, heavy SILAC lysates were labeled with a 1:1 ratio of the same reagents. The sCLIP and the TMT labeled samples were prepared in parallel with the notable exception that the TMT samples were not combined until later in the sample preparation workflow due to the requirement that the TMT labeling must occur at the peptide level. In contrast, sCLIP reagents allow for the combination of labeled samples prior to proteomic preparation (**Figure 6A**).

By combining the light SILAC 1:10 samples with the heavy SILAC 1:1 samples pairwise in a 1:4 stoichiometry, we aimed to compare the relative ratio compression, due to precursor co-isolation, for TMT- and sCLIP-labeled samples. Consistent with prior reports of MS2-based isobaric reporter ion quantification[90], we observe marked compression of the reporter ion intensity ratios from the expected log2 L/H ratio of 3.32 to 1.479 and 1.772 for sCLIP and TMT respectively (**Figure 6B**). The ratios for the light SILAC 1:1 samples both centered around 1, as expected due to the relative abundance of those precursor ions compared with the comparatively rarer ions from the 1:10 spike in. Consistent with the slightly higher ratio compression observed for sCLIP, we also observed a slightly increased coefficient of variance for the sCLIP samples when compared with TMT (**Figure 6C**). We ascribe these differences to the modest decrease in median reporter ion intensity observed for sCLIP compared with TMT (**Figure S16**). The slight decrease in sCLIP ratio compression and covariance was offset by the marked decreased reagent cost (**Figure 6D**) and increased coverage (**Figure S17**), when compared to TMT.
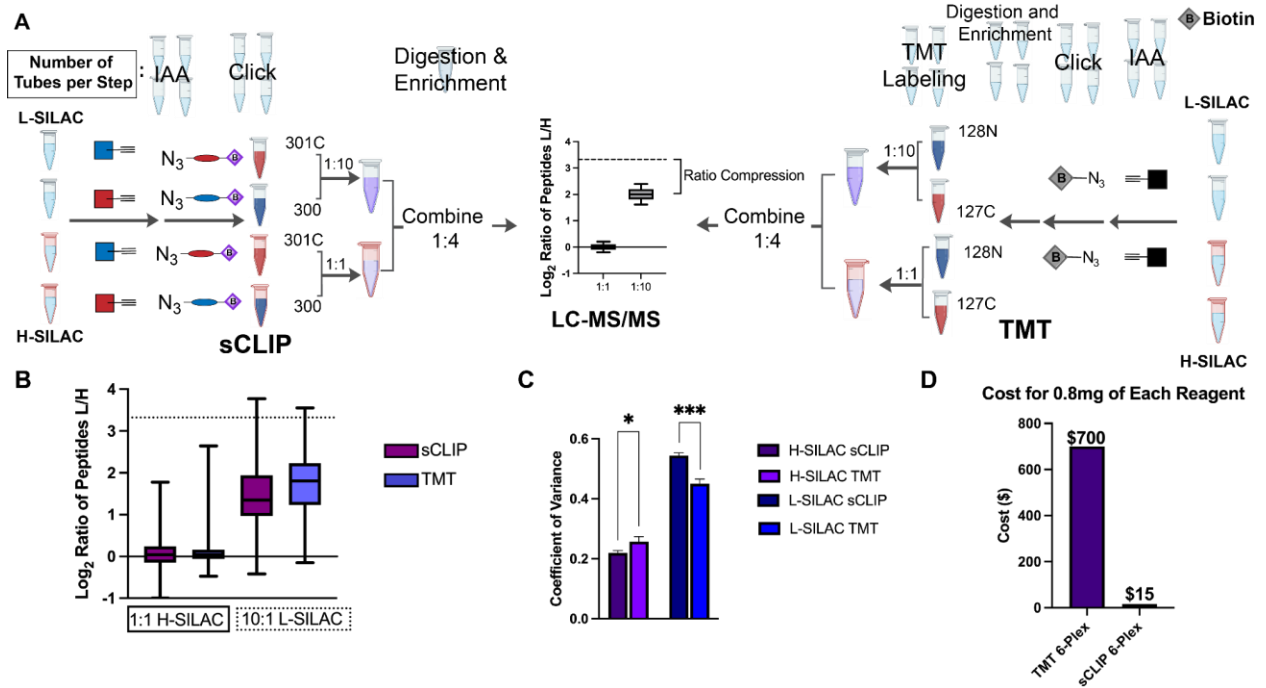
Figure 6. Comparison of sCLIP to TMT multiplexing. (A) Ratio compression workflow comparing a 2-plex set of sCLIP and a 2-plex set of TMT reagents. (B) Log2 ratio of light over heavy reporter ion intensity for sCLIP (300/301C) and TMT (127/128N) labeled peptides. Box plots display minimum, first quartile (Q1), median, third quartile (Q3), and maximum values of the sample (C) Coefficient of variance for sCLIP vs TMT tags. (D) Price comparison between commercially available 0.8mg of TMT 6-plex reagent set and estimated cost of 0.8mg of sCLIP 6-plex set. Statistical significance was calculated with a two-tailed student's t-test, *p < 0.05, **p < 0.01, ***p < 0.001, and NS p > 0.05. All MS data can be found in **Table S6**.

sCLIP enables proteome-wide multiplexed covalent fragment screening

A key advantage of the sCLIP approach compared with TMT is it allows for samples to be combined early in the sample preparation workflow, which streamlines sample preparation,

particularly for studies that require peptide- rather than protein-quantification. Cysteine chemoproteomics exemplifies one such area where peptide-level quantification is frequently used to evaluate cysteine labeling, either due to covalent alkylation by a druglike molecule or to changes in cysteine oxidation state. Isobaric labeling enabled multiplexing is particularly useful for covalent compound screening, as exemplified by the large library screen reported recently by Kuljanin and colleagues[22]. Thus, we opted here to test whether the sCLIP isobaric multiplexing platform would extend to covalent small molecule screening at cysteine residues (**Figure 7A**).

To enable high confidence benchmarking, we first generated two rigorously curated datasets of cysteines expected to be modified by the electrophilic scout fragment **KB02**[23] (**Figure S1** and **Figure 7B**), which has been use quite extensively in prior studies for landscaping the ligandable cysteinome[3,25,48,63,91]. Using precursor (MS1) quantification and following the general cysteine small molecule screening workflow shown in **Figure S18A**, we analyzed the **KB02** targets in parallel comparing two pairs of isotopically labeled capture handles, newly synthesized sCLIP reagents **10** and **14** (**Figure 2** and **Figure S18B**) and our previously reported heavy and light azido-biotin reagents (**Figure S1**)[55]. Across three biological replicates, sCLIP MS1 analysis quantified 8876 unique cysteines (**Figure S18C**). Of these, 1,421 cysteines were observed to have elevated ratios (Log_2 (DMSO/**KB02**) ratios > 2) indicative of compound labeling. Comparable coverage and precursor ion ratios were observed for samples prepared using heavy/light biotin-azide reagents (**Figure S18D**). For the sCLIP reagents, spike in experiments yielded ratios consistent with expected values (**Figure S18E**). High concordance was observed for those cysteines with elevated ratios, indicative of cysteines liganded by **KB02**, both for the sCLIP-Biotin-azide comparison and in benchmarking with previously reported datasets aggregated by CysDB, (**Figure S18F** and **Figure S18G**).

With **KB02**-ligandable dataset in hand, we next transitioned to multiplexed isobaric sample preparation with fragment-based quantification. In parallel, we treated samples treated in triplicate with **KB02** (500 uM) and duplicate with vehicle (DMSO), which were then subjected to IAA labeling

with one of three capping agents followed by click conjugation with one of five sCLIP reagents (**16-21**), affording five total isobaric samples. After labeling the samples were pooled and subjected to our established SP3-based sample preparation workflow followed by streptavidin enrichment. LC-MS/MS analysis using FAIMS was paired with a custom FragPipe workflow to generate summary reports of reporter ion intensity for identified cysteines (**Figure 7A** and **Figure 7B**). A total of 9011 total cysteines were identified across all analyzed samples and 1634 had $\log_2$ (DMSO/KB02) ratios > 1 (**Table S6**). We ascribe our slightly reduced coverage, when compared with the samples analyzed using MS1-based quantification, to the increased resolving power required for isobaric sample acquisition.

Benchmarking against our MS1-based sCLIP dataset (**Table S6**) revealed high concordance between the cysteines identified as ligandable using both methods (**Figure 7C**), albeit with a slight shift in absolute ratios detected for the samples analyzed with MS2-based quantification, likely due to ratio compression. Motivated to further increase the throughput of data acquisition and to enable SAR studies within the same sample, we next compared our **KB02** triplicate samples (three compound treated channels) with singlet preparation (single compound treated sample) (**Figure S19**). Gratifyingly, comparison of single vs multi-channel analysis for KB02-treated cell lysates revealed good concordance between both approaches with an r^2 = 0.4823 (**Figure 7D**).

As **KB02** has been extensively analyzed in the literature, we also opted to extend these analyses to datasets generated by previous studies[3,25,63,883,25,48,63,91], as aggregated by our recently reported CysDB database[48]. While there are a number of potential limitations that complicate such cross-dataset comparisons, including differences in sample preparation workflows (e.g. lysis conditions), choice of cell lines, and other sources of variability (e.g. software used for data analysis and criteria for data filtration), our prior work and MS1 analysis (**Figure S18G**) indicated that a robust subset of ligandable cysteines are highly reproducible across datasets. To account for differences in criteria used to flag a cysteine as ligandable, we chose to

prepare two curated datasets from CysDB, first a set of high confidence cysteines labeled by **KB02** (210 total cysteines), as identified by at least three independent studies, and a second of equally high confidence cysteines not labeled by KB02 (1476 total cysteines). Comparison of the sCLIP ligandable and non-ligandable cysteines to this high confidence subset revealed generally very strong concordance ~70% and ~95% for the ligandable and non-ligandable subsets, respectively (**Figure 7E**).

Having established that isobaric sCLIP can faithfully capture cysteines modified by electrophilic compounds, we next opted to extend sCLIP to two additional compounds (**Figure 7B**), **SO67** and trifluoromethoxy carbonylcyanide phenylhydrazone **(FCCP)**. As **SO67** incorporates the generally cysteine-reactive chloroacetamide electrophile, we expected that it to exhibit comparable proteome-wide reactivity to that observed for **KB02**, which would allow us to further test the generalizability of sCLIP for cysteine chemoproteomics. As a potent uncoupling agent[92], **FCCP** is widely utilized to study mitochondrial respiration. While the malononitrile hydrazone moiety has some structural parallels to known covalent reversible electrophiles, including nitrile[93–95] and cyanoacrylate/acrylamide groups[96–99], FCCP's functions have been ascribed to protonophore activity, and its potential cysteine reactivity remains unexplored.

Following the same workflow that we used to profile **KB02** (**Figure 7A**), we subjected **FCCP** and **SO67** to sCLIP analysis, which revealed 6603 and 6613 total identified cysteines, respectively (**Figure S20** and **Figure S21**). As with **KB02**, comparison between singlet and triplicate analysis (**Figure S19**) revealed good concordance (**Figure 7D and Figure S22**). Stratification of the unique and overlapping cysteines labeled by each compound revealed a unique subset of cysteines targetted by **FCCP**, when compared to the chloroacetamide-containing compounds **KB02** and **SO67** (**Figure S23**). Cysteines modified that were unique to **FCCP** include those found in mitochondrially annotated proteins, including isocitrate dehydrogenase enzymes (Cys 185 in IDH3B and Cys 308 in IDH28), and Cys57 in the ADP/ATP carrier protein ANT2 (AAC2 also known as ADT2 or SLC25A5); notably of the three cysteines identified in ANT2 only

Cys57 was labeled by FCCP (**Figure 7G**). This latter observation is particularly intriguing given ANT2's established function in mitochondrial uncoupler-induced proton leak[100] and the previous implication of post-translational acetylation of ANT2 in activating uncoupling activity[101–103]. We observe that Cys57 is located on the first loop facing the matrix, as modeled by AlphaFold[104,105] and resolved in the structure of the bovine orthologue of ANT1 (PDB-2C3E) (**Figure 7H**). Supporting the possibility that covalent modification of Cys57 by **FCCP** could contribute to proton leak, prior crosslinking studies implicated this cysteine in bovine ANT2 as the primary site for maleimide labeling in an M-state dependent manner, and which inhibited ADP transport[106]. Cys57 is additionally conserved across mouse and rat orthologues.

Given the unprecedented nature of FCCP's cysteine-reactivity, we also validated the labeling in a competitive gel-based ABPP assay We find that FCCP treatment affords a substantial decrease in IA-Rhodamine labeling, which is near-completely reversed by gel-filtration after FCCP compound labeling, with negligible effect observed for gel-filtration prior to FCCP labeling (**Figure 7I**). These findings support that FCCP functions as a covalent reversible cysteine-reactive electrophile, which is consistent with the reversibility of its leak inducing activity.
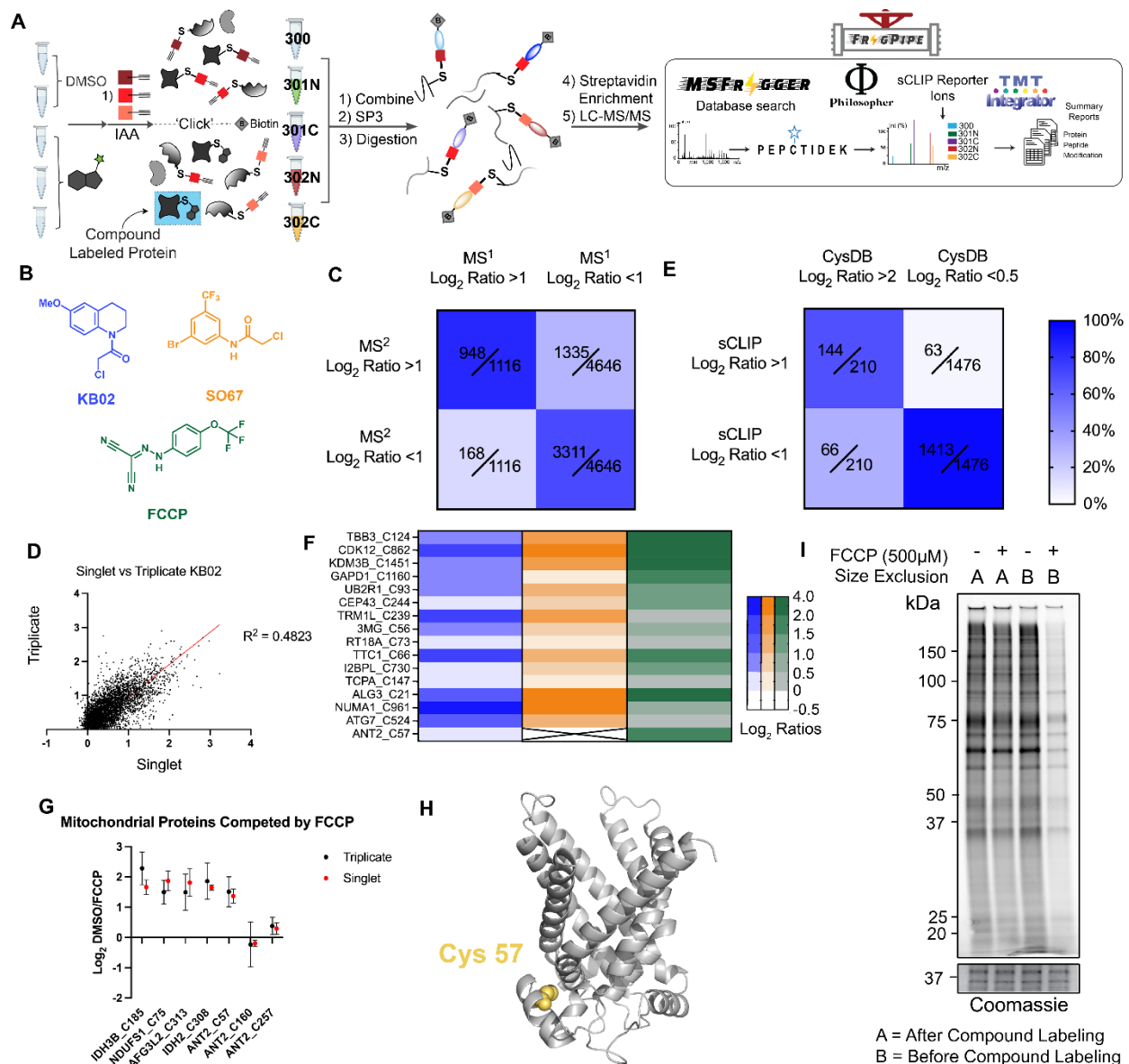
Figure 7. sCLIP is compatible with covalent fragment electrophile screening. (A) Workflow for cysteine profiling using a 5-plex sCLIP platform. In this workflow two aliquots of cell lysate are treated with DMSO and three aliquots are treated with compound. The treated lysates are then treated with one of three isotopically differentiated IAAs followed by click with one of the 5-plex reagents complementary to the IAA used. Upon combination the sample is then subjected to SP3 cleanup, trypsin digestion, streptavidin enrichment, and LC-MS/MS analysis, followed by computational analysis using FragPipe, revealing different ratios of reporter ions for each peptide.

(B) Compound structures. (C) Concordance between the log2 ratios of cysteines identified using our MS1 analysis (x-axis) and our MS2 analysis (y-axis). (D) Log2 of the ratios for cysteines at the MS1-level divided by the MS2-level shown for all cysteines, cysteines with a log2 ratio greater than 0, and cysteines with a log2 ratio less than 0. (E) Concordance between the log2 ratios of cysteines identified using three channels (x-axis) and single channel (y-axis). (F) Log2 of the ratios for cysteines identified in the triplicate data divided by the singlet data shown for all cysteines. (G) Comparison of $\log_2$ ratios of cysteines identified in KB02 (blue), SO67 (orange), and FCCP (Green) datasets. (H) Comparison of the $\log_2$ ratios of cysteines from select mitochondrial annotated proteins. (I)Structure of ANT2 as modeled with AlphaFold (P05141) with cysteines identified in our FCCP dataset labeled green. (J) Competitive gel-based ABPP assay to visualize FCCP cysteine reactivity and reversibility. Lysates were labeled with FCCP followed by IAA and click conjugation to rhodamine azide. Samples are subjected to gel filtration either prior to or after FCCP labeling. Increase in the in gel fluorescence for samples treated after FCCP labeling supports covalent reversibility. Coomassie Brilliant Blue used as protein loading control. All MS data can be found in **Table S7**.

DISCUSSION

By establishing a streamlined and high yielding synthetic route to solid phase-compatible DADPS-Fmoc building blocks, we enable the facile synthesis of customized chemoproteomics capture reagents, termed sCLIP reagents. These sCLIP reagents feature four key functionalities, biotin for enrichment, azide groups for click chemistry conjugation, a chemically cleavable DADPS linker for release of captured peptides, and isotopic labeling via low-cost isotopically labeled amino acid building blocks. Given the widespread adoption of DADPS groups in chemoproteomic capture reagents, which is likely due to improved performance compared with other cleavable handles[71], we expect that our new synthetic routes to obtain these reagents will have widespread

applications. The synthetic advances afforded by the DADPS-Fmoc building blocks are particularly noteworthy considering the low yielding and complex synthetic routes typically required to obtain similar reagents, together with the very limited availability of commercially available isotopically enriched DADPS-based capture reagents for quantitative chemoproteomics.

Enabled by our streamlined synthesis, we obtained a panel of 13 total sCLIP reagents (Figure S1), in high yield and purity. These reagents performed comparably to our established biotin-azide platform[55]. FragPipe-enabled PTM-Shepherd diagnostic feature detection[73] allowed us to predict the likely fragmentation patterns for a panel of six reagents and revealed the formation of signature dihydrooxazolium ions, generated from ß-azido-alanine-based reagents. By combining the dihydrooxazolium ion species's high intensity and precursor modification state specificity with a customized version of Philosopher, we generated a six-plex isobaric reagent set in which the balancer is encoded by isotopically labeled IAA cysteine capping agents and the reporter encoded by the sCLIP enrichment handle. This discovery, which was enabled by diagnostic ion mining, points towards untapped opportunities for mining chemoproteomics datasets to uncover additional fragment ions, including likely some already identified by our current reagent panel, with suitable properties for proteomic sample multiplexing, including via isobaric applications and other forms of sample barcoding. Key areas for future growth include increased multi-plexing capabilities, beyond six-plex. Such future reagent sets will benefit from increased reporter ion intensity.

Despite comparatively modest six-plex multiplexing capabilities afforded by this current iteration of the sCLIP platform, several features distinguish the sCLIP isobaric reagent set from other commercially available reagents. While a single prior report has demonstrated the utility of click chemistry in the synthesis of isobaric reagents[87], to our knowledge, formation of the isobaric tag in situ via bioorthogonal chemistry, with the balancer and reporter incorporated on separate labeling agents is unprecedented. Here we demonstrate the utility of this approach for cysteine chemoproteomic sample preparation and acquisition, as shown by our screens of three covalent

fragments. sCLIP-enabled screens showed high accuracy in identifying cysteines labeled by electrophilic compound KB02, both when compared to MS1-based datasets generated in parallel and to previously reported datasets[3,22,25,63,91], as aggregated by our CysDB database[48]. Extension of the sCLIP platform to study two additional electrophiles revealed the heretofore unreported covalent reversible cysteine-reactivity of the mitochondrial uncoupling agent FCCP. While we should note that these studies were conducted in cell lysates and may not translate to bulk cell or mitochondria analysis, we expect that this finding may shed light on new modes of action for FCCP, beyond its established protonophore activity as well as insights into the MOA for other molecules featuring this electrophile, including the vasodilator Levosimendan[107,108].

While cysteine chemoproteomic studies are readily conducted using TMT-based multiplexing platforms[22,25], a strength of the sCLIP approach is that the samples can be combined immediately after the click biotinylation step. This early combine substantially reduces the number of parallel sample manipulation steps and streamlines the overall workflow, as shown in **Figure 6A**. In principle similar, somewhat similar six-plex enrichment based multiplexing is possible when cysteine-reactive tandem mass tags are combined with commercially available anti-TMT resin[67]. However, sCLIP reagent's comparatively modest cost, hydrolytic stability for improved storage, and likely generalized compatibility with a range of protein and peptide-functionalization chemistries are features not built into such an anti-TMT-based approach. Furthermore, the comparatively low collision energy required for sCLIP may prove useful for analysis of peptides with labile post translational modifications, such as glycans. An additional key area in which we can envision unique applications of sCLIP is for applications uniquely enabled through separating the balancer and reporter. Notable examples where such chemistry will likely prove useful include applications relying on combined inter- and intra-sample comparisons, most notably in redox proteomics, particularly for studies aimed at tissue- and subcellular-stratification of the redoxome[14,15,17,109,110].

Looking to the future, we can envision areas for future growth and reagent development. Our current study relies on MS2-quantification, which while high throughput and accurate, suffers from unavoidable ratio compression. To address this limitation, here we implemented acquisition using a FAIMS device to reduce ratio compression. In future generation sCLIP reagents, we plan to incorporate compatibility with synchronous precursor selection-real time search-LC-MS/MS/MS (SPS-RTS-MS3)[111] and increased multiplexing capacity through alternative isobaric labeling strategies, including for example those that eliminate ratio compression[112–114]. When paired with off-line sample fractionation and automated sample preparation workflows, we expect to continue to streamline the throughput, coverage, and accuracy of quantitative cysteine chemoproteomics.

Author Contributions

N.R.B. and K.M.B. conceived of the project. N.R.B. and S.O. generated reagents. S.O. performed the gel-based assay. N.R.B. and F.S. collected data. N.R.B., F.S., S.Y., D.A.P., and D.J.G.

performed data analysis. F.V.L. and D.A.P. developed software. N.R.B., S.Y., and D.A.P contributed to figures. N.R.B. and K.M.B wrote the manuscript with assistance from all authors.

Conflicts of Interest

The authors declare no financial or commercial conflict of interest.

ASSOCIATED CONTENT

Detailed methods of chemical synthesis and chemoproteomic sample preparation; Supplementary figures and tables (PDF)

Aggregated datasets for each result section (xlsx)

REFERENCES

1. Guo, W. H. *et al.* Enhancing intracellular accumulation and target engagement of PROTACs with reversible covalent chemistry. *Nat. Commun.* **11**, 1–16 (2020).

2. Gabizon, R. *et al.* Efficient Targeted Degradation via Reversible and Irreversible Covalent PROTACs. *J. Am. Chem. Soc.* **142**, 11734–11742 (2020).

3. Zhang, X., Crowley, V. M., Wucherpfennig, T. G., Dix, M. M. & Cravatt, B. F. Electrophilic PROTACs that degrade nuclear proteins by engaging DCAF16. *Nat. Chem. Biol.* **15**, 737–746 (2019).

4. Tao, Y. *et al.* Targeted Protein Degradation by Electrophilic PROTACs that Stereoselectively and Site-Specifically Engage DCAF1. *J. Am. Chem. Soc.* **144**, 18688–18699 (2022).

5.   Luo, M. *et al.* Chemoproteomics-enabled discovery of covalent RNF114-based degraders that mimic natural product function. *Cell Chem. Biol.* **28**, 559-566.e15 (2021).

6.   Słabicki, M. *et al.* Small-molecule-induced polymerization triggers degradation of BCL6. *Nature* **588**, 164–168 (2020).

7.   Lazear, M. R. *et al.* Proteomic discovery of chemical probes that perturb protein complexes in human cells. *bioRxiv* 2022.12.12.520090 (2022).

8.   Hacker, S. M. *et al.* Global profiling of lysine reactivity and ligandability in the human proteome. *Nat. Chem.* **9**, 1181–1190 (2017).

9.   Geri, J. B. *et al.* Microenvironment mapping via Dexter energy transfer on immune cells. *Science (80-.).* **367**, 1091–1097 (2020).

10.   Zanon, P. R. A., Lewald, L. & Hacker, S. M. Isotopically Labeled Desthiobiotin Azide (isoDTB) Tags Enable Global Profiling of the Bacterial Cysteinome. *Angew. Chemie - Int. Ed.* **59**, 2829–2836 (2020).

11.   Le, P. *et al.* Repurposing human kinase inhibitors to create an antibiotic active against drug-resistant Staphylococcus aureus, persisters and biofilms. *Nat. Chem.* **12**, 145–158 (2020).

12.   Shi, Y. *et al.* Thiol-based chemical probes exhibit antiviral activity against SARS-CoV-2 via allosteric disulfide disruption in the spike glycoprotein. *Proc. Natl. Acad. Sci. U. S. A.* **119**, (2022).

13.   Piazza, I. *et al.* A machine learning-based chemoproteomic approach to identify drug targets and binding sites in complex proteomes. *Nat. Commun.* **11**, 1–13 (2020).

14.   Xiao, H. *et al.* A Quantitative Tissue-Specific Landscape of Protein Redox Regulation during Aging. *Cell* **180**, 968-983.e24 (2020).

15.   Yan, T. *et al.* Proximity-labeling chemoproteomics defines the subcellular cysteinome and inflammation-responsive mitochondrial redoxome. *biorxiv* 1–27 (2023) doi:https://doi.org/10.1101/2023.01.22.525042.

16. Meng, J. *et al.* Global profiling of distinct cysteine redox forms reveals wide-ranging redox regulation in C. elegans. *Nat. Commun.* **12**, 1–13 (2021).

17. Desai, H. S. *et al.* SP3-Enabled Rapid and High Coverage Chemoproteomic Identification of Cell-State–Dependent Redox-Sensitive Cysteines. *Mol. Cell. Proteomics* **21**, 100218 (2022).

18. Flaxman, H. A., Chang, C. F., Wu, H. Y., Nakamoto, C. H. & Woo, C. M. A Binding Site Hotspot Map of the FKBP12-Rapamycin-FRB Ternary Complex by Photoaffinity Labeling and Mass Spectrometry-Based Proteomics. *J. Am. Chem. Soc.* **141**, 11759–11764 (2019).

19. Miyamoto, D. K., Flaxman, H. A., Wu, H. Y., Gao, J. & Woo, C. M. Discovery of a Celecoxib Binding Site on Prostaglandin e Synthase (PTGES) with a Cleavable Chelation-Assisted Biotin Probe. *ACS Chem. Biol.* **14**, 2527–2532 (2019).

20. Shi, H., Zhang, C. J., Chen, G. Y. J. & Yao, S. Q. Cell-based proteome profiling of potential Dasatinib targets by use of affinity-based probes. *J. Am. Chem. Soc.* **134**, 3001–3014 (2012).

21. Bateman, L. A., Zaro, B. W., Miller, S. M. & Pratt, M. R. An alkyne-aspirin chemical reporter for the detection of aspirin-dependent protein modification in living cells. *J. Am. Chem. Soc.* **135**, 14568–14573 (2013).

22. Kuljanin, M. *et al.* Reimagining high-throughput profiling of reactive cysteines for cell-based screening of large electrophile libraries. *Nat. Biotechnol.* **39**, 630–641 (2021).

23. Backus, K. M. *et al.* Proteome-wide covalent ligand discovery in native biological systems. *Nature* **534**, 570–574 (2016).

24. Resnick, E. *et al.* Rapid Covalent-Probe Discovery by Electrophile-Fragment Screening. *J. Am. Chem. Soc.* **141**, 8951–8968 (2019).

25. Vinogradova, E. V. *et al.* An Activity-Guided Map of Electrophile-Cysteine Interactions in Primary Human T Cells. *Cell* **182**, 1009-1026.e29 (2020).

26.   Wang, Y. *et al.* Expedited mapping of the ligandable proteome using fully functionalized enantiomeric probe pairs. *Nat. Chem.* **11**, 1113–1123 (2019).

27.   Suresh, B. M. *et al.* A general fragment-based approach to identify and optimize bioactive ligands targeting RNA. *Proc. Natl. Acad. Sci. U. S. A.* **117**, 33197–33203 (2020).

28.   Parker, C. G. *et al.* Ligand and Target Discovery by Fragment-Based Screening in Human Cells. *Cell* **168**, 527-541.e29 (2017).

29.   Lu, W. *et al.* Fragment-based covalent ligand discovery. *RSC Chem. Biol.* **2**, 354–367 (2021).

30.   Mortenson, D. E. *et al.* 'inverse Drug Discovery' Strategy to Identify Proteins That Are Targeted by Latent Electrophiles As Exemplified by Aryl Fluorosulfates. *J. Am. Chem. Soc.* **140**, 200–210 (2018).

31.   Mons, E. *et al.* The Alkyne Moiety as a Latent Electrophile in Irreversible Covalent Small Molecule Inhibitors of Cathepsin K. *J. Am. Chem. Soc.* **141**, 3507–3514 (2019).

32.   Byun, D. P. *et al.* Covalent inhibition by a natural product-inspired latent electrophile. *bioRxiv* (2023).

33.   Simon, G. M. & Cravatt, B. F. Activity-based proteomics of enzyme superfamilies: Serine hydrolases as a case study. *J. Biol. Chem.* **285**, 11051–11055 (2010).

34.   Shenoy, V. M. *et al.* Chemoproteomic Identification of Serine Hydrolase RBBP9 as a Valacyclovir-Activating Enzyme. *Mol. Pharm.* **17**, 1706–1714 (2020).

35.   Li, W., Blankman, J. L. & Cravatt, B. F. A functional proteomic strategy to discover inhibitors for uncharacterized hydrolases. *J. Am. Chem. Soc.* **129**, 9594–9595 (2007).

36.   Hahm, H. S. *et al.* Global targeting of functional tyrosines using sulfur-triazole exchange chemistry. *Nat. Chem. Biol.* **16**, 150–159 (2020).

37.   Lin, S. *et al.* Redox-based reagents for chemoselective methionine bioconjugation. *Science (80-.).* **355**, 597–602 (2017).

38.   Bach, K., Beerkens, B. L. H., Zanon, P. R. A. & Hacker, S. M. Light-Activatable, 2,5-

Disubstituted Tetrazoles for the Proteome-wide Profiling of Aspartates and Glutamates in Living Bacteria. *ACS Cent. Sci.* (2020) doi:10.1021/acscentsci.9b01268.

39. Ma, N. *et al.* 2 H-Azirine-Based Reagents for Chemoselective Bioconjugation at Carboxyl Residues Inside Live Cells. *J. Am. Chem. Soc.* **142**, 6051–6059 (2020).

40. Cheng, K. *et al.* Tetrazole-Based Probes for Integrated Phenotypic Screening, Affinity-Based Proteome Profiling, and Sensitive Detection of a Cancer Biomarker. *Angew. Chemie - Int. Ed.* **56**, 15044–15048 (2017).

41. Thompson, D. A., Ng, R. & Dawson, P. E. Arginine selective reagents for ligation to peptides and proteins. *J. Pept. Sci.* **22**, 311–319 (2016).

42. Weerapana, E. *et al.* Quantitative reactivity profiling predicts functional cysteines in proteomes. *Nature* **468**, 790–797 (2010).

43. Müller, S. *et al.* Target 2035-update on the quest for a probe for every protein. *RSC Med. Chem.* **13**, 13–21 (2022).

44. Carter, A. J. *et al.* Target 2035: probing the human proteome. *Drug Discov. Today* **24**, 2111–2115 (2019).

45. Batth, T. S., Francavilla, C. & Olsen, J. V. O ff -Line High-pH Reversed-Phase Fractionation for In-Depth Phosphoproteomics. *J. Proteome Res.* **13**, 6176–6186 (2014).

46. Wang, H. *et al.* An off-line high pH reversed-phase fractionation and nano-liquid chromatography-mass spectrometry method for global proteomic profiling of cell lines. *J. Chromatogr. B Anal. Technol. Biomed. Life Sci.* **974**, 90–95 (2015).

47. Yan, T. *et al.* SP3-FAIMS Chemoproteomics for High-Coverage Profiling of the Human Cysteinome**. *ChemBioChem* **22**, 1841–1851 (2021).

48. Boatner, L. M., Palafox, M. F., Schweppe, D. K. & Backus, K. M. CysDB : A Human Cysteine Database based on Experimental Quantitative Chemoproteomics. *bioRxiv* 1–46 (2023).

49. Abegg, D. *et al.* Proteome-Wide Profiling of Targets of Cysteine reactive Small Molecules

by Using Ethynyl Benziodoxolone Reagents. *Angew. Chemie - Int. Ed.* **54**, 10852–10857 (2015).

50. Tessier, R. *et al.* Ethynylation of Cysteine Residues: From Peptides to Proteins in Vitro and in Living Cells. *Angew. Chemie - Int. Ed.* **59**, 10961–10970 (2020).

51. Allouche, E. M. D., Grinhagena, E. & Waser, J. Hypervalent Iodine-Mediated Late-Stage Peptide and Protein Functionalization. *Angew. Chemie - Int. Ed.* **61**, (2022).

52. Tang, K. C., Maddox, S. M., Backus, K. M. & Raj, M. Tunable heteroaromatic azoline thioethers (HATs) for cysteine profiling. *Chem. Sci.* **13**, 763–774 (2022).

53. Cao, J. *et al.* Multiplexed CuAAC Suzuki − Miyaura Labeling for Tandem Activity- Based Chemoproteomic Pro fi ling. (2021) doi:10.1021/acs.analchem.0c04726.

54. Desai, H. S., Yan, T. & Backus, K. M. SP3-FAIMS-Enabled High-Throughput Quantitative Profiling of the Cysteinome. *Curr. Protoc.* **2**, 1–31 (2022).

55. Yan, T. *et al.* Enhancing Cysteine Chemoproteomic Coverage through Systematic Assessment of Click Chemistry Product Fragmentation. *Anal. Chem.* (2022) doi:10.1021/acs.analchem.1c04402.

56. Ong, S. E. *et al.* Stable isotope labeling by amino acids in cell culture, SILAC, as a simple and accurate approach to expression proteomics. *Mol. Cell. Proteomics* **1**, 376–386 (2002).

57. Kim, H. Y. H., Tallman, K. A., Liebler, D. C. & Porter, N. A. An azido-biotin reagent for use in the isolation of protein adducts of lipid-derived electrophiles by streptavidin catch and photorelease. *Mol. Cell. Proteomics* **8**, 2080–2089 (2009).

58. Benns, H. J. *et al.* CRISPR-based oligo recombineering prioritizes apicomplexan cysteines for drug discovery. *Nat. Microbiol.* **7**, (2022).

59. Kong, A. T., Leprevost, F. V., Avtonomov, D. M., Mellacheruvu, D. & Nesvizhskii, A. I. MSFragger: Ultrafast and comprehensive peptide identification in mass spectrometry-based proteomics. *Nat. Methods* **14**, 513–520 (2017).

60. Pino, L. K. *et al.* The Skyline ecosystem: Informatics for quantitative mass spectrometry proteomics. *Mass Spectrom. Rev.* **39**, 229–244 (2020).

61. Gao, J. *et al.* CIMAGE2.0: An Expanded Tool for Quantitative Analysis of Activity-Based Protein Profiling (ABPP) Data. *J. Proteome Res.* **20**, 4893–4900 (2021).

62. Yu, F., Haynes, S. E. & Nesvizhskii, A. I. IonQuant enables accurate and sensitive label-free quantification with FDR-controlled match-between-runs. *Mol. Cell. Proteomics* **20**, 100077 (2021).

63. Yang, F., Jia, G., Guo, J., Liu, Y. & Wang, C. Quantitative Chemoproteomic Profiling with Data-Independent Acquisition-Based Mass Spectrometry. *J. Am. Chem. Soc.* **144**, 901–911 (2022).

64. Thompson, A. *et al.* Tandem mass tags: A novel quantification strategy for comparative analysis of complex protein mixtures by MS/MS. *Anal. Chem.* **75**, 1895–1904 (2003).

65. Li, J. *et al.* TMTpro reagents: a set of isobaric labeling mass tags enables simultaneous proteome-wide measurements across 16 samples. *Nat. Methods* **17**, (2020).

66. Sun, Y. *et al.* Mitochondrial TNAP controls thermogenesis by hydrolysis of phosphocreatine. *Nature* **593**, 580–585 (2021).

67. Murray, C. I., Uhrigshardt, H., O'Meally, R. N., Cole, R. N. & Van Eyk, J. E. Identification and quantification of S-nitrosylation by cysteine reactive tandem mass tag switch assay. *Mol. Cell. Proteomics* **11**, M111.013441 (2012).

68. Chanda, P. K. *et al.* Nuclear S-nitrosylation defines an optimal zone for inducing pluripotency. *Circulation* **140**, 1081–1099 (2019).

69. Szychowski, J. *et al.* Cleavable biotin probes for labeling of biomolecules via azide-alkyne cycloaddition. *J. Am. Chem. Soc.* **132**, 18351–18360 (2010).

70. Gertsik, N. *et al.* Mapping the Binding Site of BMS-708163 on γ-Secretase with Cleavable Photoprobes. *Cell Chem. Biol.* **24**, 3–8 (2017).

71. Li, Z., Liu, K., Xu, P. & Yang, J. Benchmarking Cleavable Biotin Tags for Peptide-Centric

Chemoproteomics. *J. Proteome Res.* **21**, 1349–1358 (2022).

72. Polasky, D. A. *et al.* MSFragger-Labile: A Flexible Method to Improve Labile PTM
     Analysis in Proteomics. *bioRxiv* (2022).

73. Geiszler, D. J., Polasky, D. A., Yu, F. & Nesvizhskii, A. I. Mining for ions: diagnostic
     feature detection in MS/MS spectra of post-translationally modified peptides. *bioRxiv*
     (2022).

74. Heytler, P. G. Uncouplers of Oxidative Phosphorylation. *Methods Enzymol.* **55**, 462–472
     (1979).

75. Gao, J., Mfuh, A., Amako, Y. & Woo, C. M. Small Molecule Interactome Mapping by
     Photoaffinity Labeling Reveals Binding Site Hotspots for the NSAIDs. *J. Am. Chem. Soc.*
     140, 4259–4268 (2018).

76. Conway, L. P. *et al.* Evaluation of fully-functionalized diazirine tags for chemical
     proteomic applications. *Chem. Sci.* **12**, 7839–7847 (2021).

77. Boehm, T. L. & Showalter, H. D. H. Development of a novel silyl ether linker for solid-
     phase organic synthesis. *J. Org. Chem.* **61**, 6498–6499 (1996).

78. Randolph, J. T., McClure, K. F. & Danishefsky, S. J. Major Simplifications in
     Oligosaccharide Syntheses Arising from a Solid-Phase Based Method: An Application to
     the Synthesis of the Lewis b Antigen. *J. Am. Chem. Soc.* **117**, 5712–5719 (1995).

79. Atherton, E., Logan, C. J. & Sheppard, R. C. Peptide synthesis. Part 2.' Procedures for
     Solid-phase Synthesis using Na-Fluorenylmethoxycarbonylamino-acids on Polyamide
     Supports. Synthesis of Substance P and of Acyl Carrier Protein 65-74 Decapeptide.
     J.C.S Perkin I (1981).

80. ALBERICIO, F. & BARANY, G. Application of N,Ndimethylformamide dineopentyl acetal
     for efficient anchoring of N(alpha)-9-fluorenylmethyloxycarbonylamino acids as p-
     alkoxybenzyl esters in solid-phase peptide synthesis. *Int. J. Pept. Protein Res.* 342–349
     (1984).

81. Tucker-Schwartz, A. K., Farrell, R. A. & Garrell, R. L. Thiol - Ene click reaction as a general route to functional trialkoxysilanes for surface coating applications. *J. Am. Chem. Soc.* **133**, 11026–11029 (2011).

82. Polasky, D. A., Yu, F., Teo, G. C. & Nesvizhskii, A. I. Fast and comprehensive N- and O-glycoproteomics analysis with MSFragger-Glyco. *Nat. Methods* **17**, 1125–1132 (2020).

83. Li, K., Vaudel, M., Zhang, B., Ren, Y. & Wen, B. PDV: An integrative proteomics data viewer. *Bioinformatics* **35**, 1249–1251 (2019).

84. Abo, M., Li, C. & Weerapana, E. Isotopically-Labeled Iodoacetamide-Alkyne Probes for Quantitative Cysteine-Reactivity Profiling. *Mol. Pharm.* **15**, 743–749 (2018).

85. McAlister, G. C. *et al.* Increasing the multiplexing capacity of TMTs using reporter ion isotopologues with isobaric masses. *Anal. Chem.* **84**, 7469–7478 (2012).

86. Xiang, F., Ye, H., Chen, R., Fu, Q. & Li, L. N , N -Dimethyl Leucines as Novel Isobaric Tandem Mass Tags for Quantitative Proteomics and Peptidomics. **82**, 4624–4632 (2010).

87. Sohn, C. H. *et al.* Click chemistry facilitates formation of reporter ions and simplified synthesis of amine-reactive multiplexed isobaric tags for protein quantification. *J. Am. Chem. Soc.* **134**, 2672–2680 (2012).

88. da Veiga Leprevost, F. *et al.* Philosopher: a versatile toolkit for shotgun proteomics data analysis. *Nat. Methods* **17**, 869–870 (2020).

89. Ross, P. L. *et al.* Multiplexed protein quantitation in Saccharomyces cerevisiae using amine-reactive isobaric tagging reagents. *Mol. Cell. Proteomics* **3**, 1154–1169 (2004).

90. Hogrebe, A. *et al.* Benchmarking common quantification strategies for large-scale phosphoproteomics. *Nat. Commun.* **9**, (2018).

91. Crowley, V. M., Thielert, M. & Cravatt, B. F. Functionalized Scout Fragments for Site-Specific Covalent Ligand Discovery and Optimization. *ACS Cent. Sci.* **7**, 613–623 (2021).

92. Heytler, P. G. & Prichard, W. W. A NEW CLASS OF UNCOUPLING AGENTS - CARBONYL CYANIDE PHENYLRYDRAZON. *Biochem. Biophys. Res. Commun.* **7**, 272–

275 (1962).

93.   Berteotti, A. *et al.* Predicting the Reactivity of Nitrile-Carrying Compounds with Cysteine:
       A Combined Computational and Experimental Study. *ACS Med. Chem. Lett.* **5**, 501–505
       (2014).

94.   Owen, D. R. *et al.* An oral SARS-CoV-2 Mpro inhibitor clinical candidate for the treatment
       of COVID-19. *Science (80-.).* **374**, 1–7 (2021).

95.   Wang, X. *et al.* Nitrile-containing pharmaceuticals: target, mechanism of action, and their
       SAR studies. *RSC Med. Chem.* **12**, 1650–1671 (2021).

96.   Senkane, K. *et al.* The Proteome-Wide Potential for Reversible Covalency at Cysteine.
       Angew. Chemie - Int. Ed. **58**, 11385–11389 (2019).

97.   Miller, R. M., Paavilainen, V. O., Krishnan, S., Sera, I. M. & Taunton, J. Electrophilic
       Fragment-Based Design of Reversible Covalent Kinase Inhibitors. *J. Am. Chem. Soc*
       135, 5298–5301 (2013).

98.   Krishnan, S. *et al.* Design of Reversible, Cysteine-Targeted Michael Acceptors Guided by
       Kinetic and Computational Analysis. *J. Am. Chem. Soc* **136**, 12624–12630 (2014).

99.   Bradshaw, J. M. *et al.* Prolonged and tunable residence time using reversible covalent
       kinase inhibitors. *Nat. Chem. Biol.* **11**, 525–531 (2015).

100.   Bertholet, A. M. *et al.* Mitochondrial uncouplers induce proton leak by activating AAC and
       UCP1. *Nature* **606**, (2022).

101.   Klingenberg, M. The ADP and ATP transport in mitochondria and its carrier. *Biochim.*
       Biophys. Acta J. **1778**, 1978–2021 (2008).

102.   Brustovetsky, N. & Klingenberg, M. The Reconstituted ADP / ATP Carrier Can Mediate H
       ' Transport by Free Fatty Acids , Which Is Further Stimulated by Mersalyl *. *J. Biol. Chem.*
       269, 27329–27336 (1994).

103.   Forman, N. G. & Wilson, D. F. Dependence of mitochondrial oxidative phosphorylation on
       activity of the adenine nucleotide translocase. *J. Biol. Chem.* **258**, 8649–8655 (1983).

104. Varadi, M. *et al.* NAR Breakthrough Article AlphaFold Protein Structure Database : massively expanding the structural coverage of protein-sequence space with high-accuracy models. *Nucleic Acids Res.* **50**, 439–444 (2022).

105. Ronneberger, O. *et al.* Highly accurate protein structure prediction with AlphaFold. *Nature* **596**, (2021).

106. Hashimoto, M., Majima, E., Goto, S., Shinohara, Y. & Terada*, H. Fluctuation of the First Loop Facing the Matrix of the Mitochondrial ADP / ATP Carrier Deduced from Intermolecular Cross-Linking of Cys 56 Residues by Bifunctional Dimaleimides. *Biochemistry* **38**, 1050–1056 (1999).

107. Szilágyi, S. *et al.* The effects of levosimendan and OR-1896 on isolated hearts, myocyte-sized preparations and phosphodiesterase enzymes of the guinea pig. *Eur. J. Pharmacol.* **486**, 67–74 (2004).

108. Papp, Z., Csapó, K., Pollesello, P., Haikala, H. & Édes, I. Pharmacological mechanisms contributing to the clinical efficacy of levosimendan. *Cardiovasc. Drug Rev.* **23**, 71–98 (2005).

109. Bak, D. W., Pizzagalli, M. D. & Weerapana, E. Identifying Functional Cysteine Residues in the Mitochondria. *ACS Chem. Biol.* **12**, 947–957 (2017).

110. Bechtel, T. J., Li, C., Kisty, E. A., Maurais, A. J. & Weerapana, E. Profiling Cysteine Reactivity and Oxidation in the Endoplasmic Reticulum. *ACS Chem. Biol.* **15**, 543–553 (2020).

111. Schweppe, D. K. *et al.* Full-Featured, Real-Time Database Searching Platform Enables Fast and Accurate Multiplexed Quantitative Proteomics. *J. Proteome Res.* **19**, 2026–2034 (2020).

112. Winter, S. V. *et al.* EASI-tag enables accurate multiplexed and interference-free MS2-based proteome quantification. *Nat. Methods* **15**, 527–530 (2018).

113. Johnson, A., Stadlmeier, M. & Wühr, M. TMTpro Complementary Ion Quantification

Increases Plexing and Sensitivity for Accurate Multiplexed Proteomics at the MS2 Level.

J. Proteome Res. **20**, 3043–3052 (2021).

114.   Kozhinov, A. N. *et al.* Super-Resolution Mass Spectrometry Enables Rapid, Accurate,

and Highly Multiplexed Proteomics at the MS2 Level. *Anal. Chem* (2023)

doi:10.1021/acs.analchem.2c04742.